Journal of Catalysis **182,** 292–301 (1999)
Article ID jcat.1998.2365, available online at http://www.idealibrary.com on IDEAL®

Temperature-Programmed Reduction and XRD Studies of Ammonia-Treated Molybdenum Oxide and Its Activity for Carbazole Hydrodenitrogenation

M. Nagai,[1] Y. Goto,[2] A. Miyata,[3] M. Kiyoshi, K. Hada, K. Oshikawa, and S. Omi

Department of Advanced Materials, Graduate School of Bio-Applications and Systems Engineering, Tokyo University of Agriculture and Technology, Koganei, Tokyo 184-8588, Japan

Received March 13, 1998; revised July 20, 1998; accepted November 23, 1998

The change in the structure and composition of molybdenum nitride catalysts with cooling in a stream of ammonia or helium gas after NH_3 treating was determined using temperature-programmed reduction (TPR) and X-ray powder diffraction analyses. The relationship between the molybdenum species and the catalytic activities of the molybdenum nitride catalysts for the hydrodenitrogenation (HDN) of carbazole was discussed. MoO_2, γ-Mo_2N, and Mo metal were mainly formed during the temperature-programmed reaction of MoO_3 with ammonia at 773, 973, and 1173 K, respectively. During the TPR experiment, a portion of the adsorbed NH_x ($x = 0$–3) species caused further nitriding of the catalyst at higher temperatures. It was found that nitrogen desorption during TPR could be assigned to four types of nitrogen species: (1) NH_x adsorbed on MoO_2, (2) NH_x adsorbed on γ-Mo_2N, (3) N_2 during the transformation of γ-Mo_2N to β-$Mo_2N_{0.78}$, and (4) N_2 during the reduction of β-$Mo_2N_{0.78}$ to molybdenum metal. Purging the NH_3-treated catalyst with helium at 973 K not only removed the adsorbed NH_x and diffused nitrogen but also altered the structure of the molybdenum compounds, i.e., from γ-Mo_2N to β-$Mo_2N_{0.78}$. During the HDN of carbazole, γ-Mo_2N was the most active, followed by β-$Mo_2N_{0.78}$ for C–N hydrogenolysis, while molybdenum metal had the highest activity for hydrogenation. NH_3-treated MoO_2 was much less active for both C–N hydrogenolysis and hydrogenation during carbazole HDN. From these results, the C–N hydrogenolysis sites were most likely located on small nitrogen deficient particles and crystallites of the molybdenum nitrides. The hydrogenation sites were located on the surface grain boundary of molybdenum metals.

INTRODUCTION

The removal of nitrogen compounds from petroleum products is deemed more difficult than the removal of sulfur compounds. Increasing interest has developed in exploring the catalytic properties of molybdenum nitrides for hydrodenitrogenation (HDN) in the hydroprocessing of petroleum feedstocks (1–10). Oyama and co-workers (1, 2) reported that unsupported molybdenum nitrides offered an interesting alternative to existing HDN catalysts and exhibited much higher selectivity for the formation of aromatic products from quinoline. Bell and co-workers (3) reported that bulk γ-Mo_2N was more active for the C–N hydrogenolysis of 1,2,3,4-tetrahydroquinoline to 2-propylbenzene during the HDN of quinoline when compared to the sulfided $NiMo/Al_2O_3$ catalyst. Thompson *et al.*(4) studied the HDN of pyridine over γ-Mo_2N and reported that the molybdenum nitride was more active than sulfided $CoMo/Al_2O_3$ catalysts (per Mo atom), having better selectivity of carbon–nitrogen bond hydrogenolysis. NH_3-treated molybdena–alumina was also reported to exhibit high activities for hydrodenitrogenation (5–8) and hydrodesulfurization (11, 12). Much less attention, however, has been given to determining the effects of purging and cooling gas after NH_3 treating on the structures, compositions, and activities of the molybdenum nitrides. Furthermore, few reports discuss the relationship between molybdenum species generated by NH_3 treatment and catalytic activity for HDN, although the NH_3-treated catalyst contained several adsorbed nitrogen species when cooling from treating temperature to room temperature in flowing ammonia (13–16).

For characterization of the NH_3-treated molybdenum oxides, temperature-programmed reduction (TPR) with hydrogen (13, 17–19) is a useful technique for determining the reactivity of adsorbed nitrogen and molybdenum species in molybdenum catalysts treated with ammonia at various temperatures. The release of nitrogen and ammonia gases from the catalyst at various desorption temperatures in the TPR profiles provides information on the molybdenum species of the catalysts. Moreover, a combination of X-ray powder diffraction (XRD) with the TPR measurement for the catalysts would provide more detailed information on the structure and compositions of the molybdenum nitrides

[1] To whom correspondence should be addressed.
[2] Current address: Denki Chemical Kogyo Co., 6 Goi-minami-Kaigan, Ichihara, Chiba 290-8588, Japan.
[3] Current address: Casio Computer Co., Ltd., Sakae Machi, Hamura, Tokyo 205-8555, Japan.

0021-9517/99 $30.00

as well as the oxidic and metallic structures. It is important to establish the changes in the structure and composition of the catalysts with adsorbed NH_x ($x = 0$–3) species during TPR and to understand the effects of the cooling gases on the catalytic activity and composition of the NH_3-treated catalysts. This paper covers the following three topics: (1) the changes in structures, compositions, and activities of the NH_3-treated molybdenum oxides with adsorbed nitrogen species during TPR; (2) the effect of the cooling gases (ammonia and helium) on the formation of molybdenum species of the catalysts after NH_3 treating; and (3) the relationship between the molybdenum species and the catalytic activity of the NH_3-treated catalysts for the HDN of carbazole.

EXPERIMENTAL

Reagents and Catalysts

Hydrogen and helium (99.9999%) were dried using an Oxiclear purifying trap and an OM-1 indicating purifier trap (Supelco, Inc.) prior to use. Ammonia (99.99%) was used without further purification. A 97.1% MoO_3/Al_2O_3 sample was prepared using a mixture of MoO_3 and alumina hydrogel and calcined in air at 823 K for 3 h (Nikki Chemical Co.). γ-Al_2O_3 (2.9%) served as a binder to maintain durability and to prevent crumbling of the catalyst at the operating pressure of 10.1 MPa. The oxidic catalyst was packed on a fritted plate in a quartz microreactor, which consisted of a 20-mm-long quartz tube of 10-mm-o.d., with 50-mm-long 6-mm-o.d. quartz tubes attached at both ends. The oxidized precursor was treated with ammonia at 49.6 μmol s^{-1} from 573 to 773 K (suffix notation, -L), 973 K (-M), and 1173 K (-H) at a rate of 0.0167 K s^{-1} (SV of 3822 h^{-1}) and held in flowing ammonia (49.6 μmol s^{-1}) at the treatment temperature for 3 h. After NH_3 treatment, two alternative methods of treatment were performed. In the first treatment the catalyst was cooled to room temperature in flowing ammonia (NH catalyst), while in the second, the catalyst was purged with helium (11.2 μmol s^{-1}) at 973 K for 1 h and then cooled to room temperature in flowing helium (11.2 μmol s^{-1}) (HE catalyst). Abbreviated notations are as follows: NH-L denotes 97.1% Mo/Al_2O_3 treated at 773 K in flowing ammonia for 3 h followed by cooling to room temperature in flowing ammonia, while HE-H denotes 97.1% Mo/Al_2O_3 treated at 1173 K in flowing ammonia for 3 h, followed by purging with helium at 973 K for 1 h and cooling to room temperature in flowing helium. The molybdenum analysis was performed using atomic absorption spectroscopy. The specific surface area (BET) of the catalyst was measured by nitrogen adsorption using a volumetric BET apparatus (Shibata Co., P-700) after evacuation of the sample at 473 K and 10^{-2} Pa for 2 h. The concentration of alumina located near the surface of a fresh oxide and NH-M was analyzed by EPMA (Jeol, JMA-8900,WDS) under the conditions of an accelerating voltage of 15 kV and scanning speed of 0.5 μm s^{-1}. Alumina was not preferentially located at the surface and was well dispersed in the catalyst. Moreover, alumina in the catalyst was not nitrided under the pretreatment conditions, since the Al 1*s* XPS spectra were indistinguishable for the nitrided Mo/Al_2O_3 catalysts before and after the reaction. XPS spectra were measured using a Shimadzu ESCA 850 spectrometer with monochromatic Mg$K\alpha$ exciting radiation (8 kV, 30 mA).

Temperature-Programmed Reduction

Temperature-programmed reduction study was performed under *in situ* conditions after the NH_3 treating preparation. The catalysts (0.2 g), NH and HE, were heated to 373 K in flowing helium at a rate of 49.6 μmol s^{-1} for 1 h after the NH_3 treatment. The sample was then heated from room temperature to 1263 K at a rate of 0.167 K s^{-1} with a hydrogen flow of 11.2 μmol s^{-1}. The gases desorbed from the sample were monitored on-line using a quadrupole mass spectrometer (ULVAC MSQ-150A) equipped with a variable-leak valve heated by heating tape at 423 K. The desorption rates of N_2 ($m/z = 28$), H_2 ($m/z = 2$), H_2O ($m/z = 18$), and NH_3 ($m/z = 15$) gases were calculated using calibration curves for each gas. The spectra of the gases were deconvoluted by curve-fitting (Origin, Microcal Co.) of the data transferred from the quadrupole mass spectrometer.

X-Ray Powder Diffraction

Since the compositions of the catalysts changed during TPR, the compositions of the intermediates and final products were measured using XRD. The preparation conditions of the catalyst were the same as those for the separate TPR experiments. X-ray powder diffraction analysis was performed with Ni-filtered Cu$K\alpha$ radiation ($\lambda = 0.15418$ nm) with a Rigaku X-ray diffractometer operating at a scanning speed of 2° min^{-1} from $2\theta = 5°$ to 120°. Patterns were identified by comparison to the following JCPD standards: MoO_3 (35–609), MoO_2 (32–671), γ-Mo_2N (25–1366), β-$Mo_2N_{0.78}$ (25–1368), and Mo metal (42–1120). The crystallite size, d_c, was determined using the Scherrer equation, $d_c = 0.9\lambda/(B\cos\theta)$, where λ is the wavelength of the X-radiation, B is the full width at half-maximum corrected for instrumental broadening, and θ is the Bragg angle of the diffraction peak.

CO Chemisorption

The quantity of CO chemisorbed on the surface of the catalysts, passivated in 1.0% O_2 in helium at room temperature for 12 h, was determined by a conventional volumetric analysis (Coulter Co., Omnisorp 100CX). Before measuring the CO uptake, the sample was first pretreated in a stream of helium at 723 K for 2 h and reduced in flowing

hydrogen at 673 K for 2 h. After the reduction, the catalyst was degassed at 10^{-2} Pa and at 673 K for 1 h and then slowly cooled to room temperature in a vacuum. The first CO isotherm was taken at increasing CO pressure following evacuation at room temperature for 1 h, and the second isotherm was taken in a similar manner. The amount of irreversible CO uptake was obtained from the difference between the two isotherms, which were extrapolated to zero pressure.

Activity Measurement for HDN of Carbazole

The HDN of carbazole on the NH and HE catalysts was conducted using a down-flow fixed-bed microreactor in a high-pressure flow system. The microreactor used was a 325-mm-long stainless steel tube of 17.3-mm-o.d. and 3.2 mm thickness. The granular catalyst (2.0 g) (0.85–1.70 mm) was held in place in the middle of the reactor by interposing it between stainless steel bars, engraved with spiral grooves. Before introduction of the feed to the reactor, the catalyst was heated at 773 K with hydrogen for 1 h and then cooled to the reaction temperature. The liquid feed, consisting of 1.50 mmol% carbazole dissolved in xylene, was introduced into the reactor at 20 ml h^{-1} with hydrogen at a rate of 74.4 μmol s^{-1} at 573 K and 10.1 MPa. The liquid reaction products were separated from gaseous products such as hydrogen, ammonia, and other products having boiling points lower than the xylene solvent in the high-pressure separator. The rates of C–N hydrogenolysis and hydrogenation of carbazole were calculated through the formation of the denitrogenated compounds and hydrogenated compounds (20), respectively, and are reported as molecules h^{-1} m^{-2}. Reaction products were quantitatively analyzed using an FID gas chromatograph with 2% Silicone OV-17 (20).

RESULTS AND DISCUSSION

BET Surface Area

The surface areas of the NH and HE catalysts are shown in Table 1. The surface area of the HE catalyst increased from 1.1 to 59 m^2 g^{-1} after NH_3 treatment at 773 K for the fresh sample, but decreased to 18 m^2 g^{-1} as the NH_3 treatment temperature increased from 773 to 1173 K. For the NH catalysts, the surface area showed the same trend of decreasing surface area with increasing treating temperature for the HE catalysts. The NH catalysts had a higher surface area than the HE catalysts at the same NH_3 treating temperature. Crystallite sizes were measured using XRD. The crystallite size of the NH catalysts was smaller than that of the HE catalysts. The average crystallite size of molybdenum metal for the NH-H and HE-H catalysts was 17 nm (calculated using the Mo(110) reflection). Table 1 shows that for all of the materials, the crystallite size is smaller than the particle size, indicating that the particles are polycrystalline agglomerates. The NH_3 treatment at 1173 K lowered the surface area in flowing ammonia and helium because of sintering of the catalysts at high temperature.

TABLE 1

Surface Area and CO Uptake of NH_3-Treated Catalysts

	Catalysts[a]					
	773		973		1173	
NH_3 treating temperature (K):	NH	HE	NH	HE	NH	HE
Surface area (m^2 g^{-1})[b]	66	59	33	18	8	6
Particle size, d_p (nm)[c]	14	16	19	35	80	107
N[d]/Mo[e]	0.16	0.17	0.33	0.40	0.86	0.03
Crystallite size, d_c (nm)	3.86	8.05	2.71	3.27	17.3	17.9
Main phase (XRD analysis)	MoO_2 (111)	MoO_2 (111)	γ-Mo_2N (111)	β-$Mo_2N_{0.78}$ (111)	Mo (110)	Mo (110)
$d_p d_c^{-2}$	0.93	0.24	2.6	3.3	0.27	0.33
Total CO (μmol g^{-1})	14.6	22.0	84.4	23.4	3.7	12.4
CO irreversible (μmol g^{-1})	5.7	12.4	43.8	10.9	1.1	4.3
Rato of irreversible to total	0.39	0.56	0.52	0.47	0.30	0.35
Atoms of CO_{total} (10^{-14} cm^{-2})	0.149	0.224	2.82	0.783	0.37	1.24
Atoms of CO_{irr} (10^{-14} cm^{-2})	0.058	0.127	1.47	0.365	0.11	0.431

[a] The sample (NH) was cooled in flowing NH_3 to room temperature after a fresh MoO_3 sample nitriding at 773 (L), 973 (M), and 1173 K (H). The sample (HE) was cooled in flowing He to room temperature after purging with helium at 973 K for 1 h.

[b] Evacuated at 473 K and at 1 Pa; fresh 97.1% MoO_3/Al_2O_3, 1.1 m^2 g^{-1}.

[c] Particle size $d_p = 6/S_g\rho$, where S_g is the BET surface area, and ρ is the density of the material here taken to be 6.5, 9.5, and 9.3 g cm^{-3} for MoO_2, γ-Mo_2N, and Mo metal, respectively.

[d] Desorption of N_2 and NH_3 above 973 K in TPR.

[e] Atomic absorption.

NH_3-Cooled Nitrided Catalysts

The TPR profile for the NH-L catalyst is shown in Fig. 1a. Desorption of nitrogen, ammonia, and water was observed. The profile showed two large desorption peaks of nitrogen at temperatures of 877 K and above 1253 K with a small desorption peak at 1010 K. A small peak of ammonia at around 800 K indicated that ammonia was released in the reaction of adsorbed nitrogen species with hydrogen (21–27) as well as the desorption of adsorbed NH_3 on molybdenum species and Al_2O_3 (13). In order to elucidate the effects of adsorbed NH_x on the surface molybdenum species during TPR, the changes in the catalyst composition were studied by interrupting the temperature program at the corresponding labeled points (e.g., A, B, C in Fig. 1a). The XRD patterns of the NH-L catalyst are shown in Fig. 2. The XRD data of the as-prepared NH-L catalyst (A) showed the presence of MoO_2 without molybdenum nitrides during treatment at 773 K. Molybdenum oxides were converted to γ-Mo_2N and β-$Mo_2N_{0.78}$ at 1075 K (Point B in Fig. 1a) with adsorbed NH_x, which remained on the as-prepared NH-L during cooling with ammonia from the NH_3 treating temperature to room temperature. A portion of the adsorbed NH_x species was consumed to form molybdenum nitrides while the remaining species desorbed as nitrogen gas at 877 K. Consequently, the nitrogen desorption at 877 K is due to the reaction of adsorbed NH_x with H_2 on MoO_2 and γ-Mo_2N. Molybdenum nitrides were not observed by XRD at room temperature and 573 K during the treatment of MoO_3 with ammonia at 773 K but occurred with adsorbed NH_x above 773 K during TPR. Further heating of the NH-L catalyst to 1253 K (C) during TPR formed a molybdenum metal (110) phase. Although the crystallite size ($MoO_2(\bar{1}11)$) from the XRD pattern for the as-prepared NH-L was 3.86 nm in Fig. 2, the NH-L catalyst at 1253 K (C) was considerably greater (14 nm). Thus, the TPR process increased the crystallite size of NH-L through the structural changes. In addition, water was desorbed above 800 K for the NH-L catalyst during TPR. Since the O/Mo ratio for NH-L was 0.85 in Table 2, molybdenum oxides remained in the catalyst treated with ammonia at 773 K.

The TPR profile for the NH-M catalyst shows three distinct desorption peaks of nitrogen at 897, 1097, and 1197 K

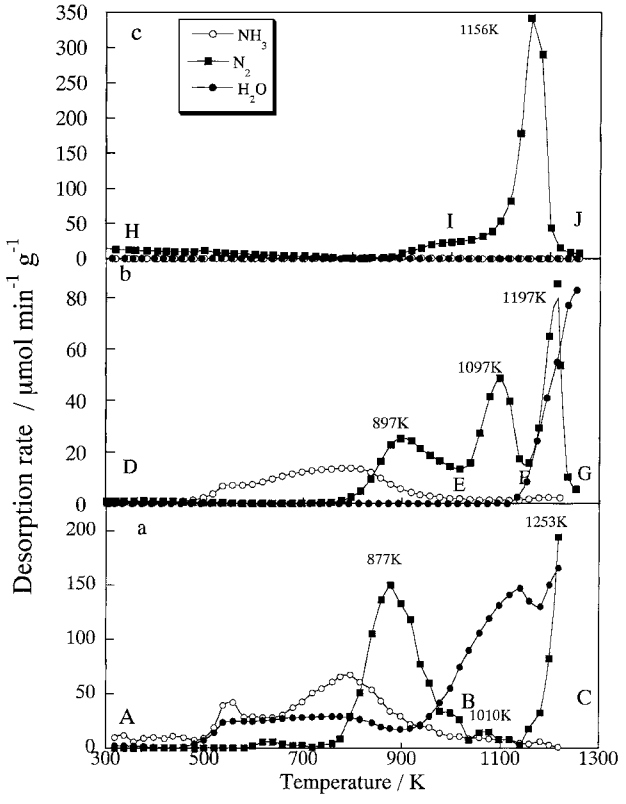

FIG. 1. TPR profiles of (a) NH-L, (b) NH-M, and (c) NH-H catalysts.

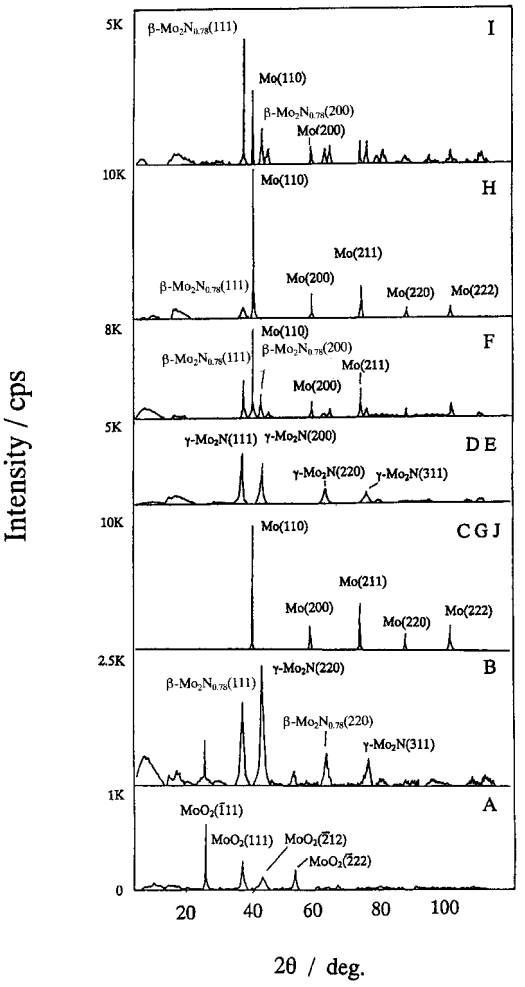

FIG. 2. The XRD spectra of the (A) as-prepared, (B) intermediates of, and (C) final compounds of NH-L catalyst; the (D) as-prepared, (E, F) intermediates of, and (G) final compounds of NH-M catalyst; and the (H) as-prepared, (I) intermediates of, and (J) final compounds of NH-L, NH-M, and NH-H catalysts during TPR.

TABLE 2

The Amount of N_2 Desorption in the TPR Profiles with Deconvolution

Catalyst	N_2 desorbed (μmol g^{-1}) (a)	(b)	(c)	(d)	Desorbed (mmol g^{-1}) N_2[a]	NH_3	Total N	N/Mo[b] ratio	H_2O desorbed (mmol g^{-1})	O[c]/Mo ratio
NH-L	68 (875)	12 (940)	9 (1060)	90 (1250)	0.099	0.72	0.918	0.16	5.7	0.85
NH-M	136 (875)	225 (940)	199 (1095)	321 (1210)	0.52	0.483	1.52	0.33	0.741	0.10
NH-H	0	136 (940)	388 (1070)	2476 (1160)	3.0	0.040	5.88	0.86	0.177	0.02
HE-L	0	0	0	498 (1199)	0.498	0.139	1.11	0.17	2.18	0.32
HE-M	0	0	789 (1087)	506 (1174)	1.30	0.133	2.72	0.40	1.16	0.17
HE-H	0	0	115 (1057)	2 (1174)	0.117	0	0.234	0.03	0.417	0.06

Note. Numbers in parentheses denote N_2 peak/K.
[a] N_2: on a basis of N_2 desorbed at more than 973 K during TPR.
[b] Atomic absorption.
[c] Formation of water from room temperature to 1275 K.

in Fig. 1b. The XRD analysis shows that the as-prepared NH-M catalyst (D) and the catalyst heated to 1017 K (E) consisted of γ-Mo_2N, as shown in Fig. 2. Nitrogen desorbed at 897 K for NH-M and at 877 K for NH-L was attributed to the release of nitrogen gas in the reaction of adsorbed NH_x with hydrogen on MoO_2 and γ-Mo_2N. In the TPR profile of NH-M, one desorption peak at 897 K was deconvoluted to two peaks for the release of nitrogen, i.e., at 875 K (MoO_2) and 940 K (γ-Mo_2N) in Table 2, as will be mentioned later, although the peak apparently consisted of one peak for NH-M during TPR. Furthermore, since NH-M contained both β-$Mo_2N_{0.78}$ and molybdenum metal at 1158 K (F) in Fig. 2, the desorption peak centered at 1097 K arose from the release of nitrogen gas during the transformation of γ-Mo_2N into β-$Mo_2N_{0.78}$. The catalyst, which was heated to 1257 K (G), was composed of molybdenum metal. The desorption peak at 1197 K is due to the release of nitrogen during the reduction of β-$Mo_2N_{0.78}$ to molybdenum metal. The presence of β-$Mo_2N_{0.78}$, as seen at the peak of 1097 K, indicated the formation of molybdenum metal from γ-Mo_2N via β-$Mo_2N_{0.78}$. Water was released slightly from NH-M above 1137 K since the O/Mo ratio was only 0.1.

The TPR profile for the NH-H catalyst is shown in Fig. 1c. The NH-H catalyst had a large peak of nitrogen desorption at 1156 K with a tailing peak at around 1000 K. As shown in Fig. 2, molybdenum metal (H) was transformed into the mixture (I) of molybdenum metal and β-$Mo_2N_{0.78}$ from 17.3 nm (Mo (110)) into 3.5 nm (β-$Mo_2N_{0.78}$ (111)) in crystallite size up to about 1000 K (I) by nitriding with adsorbed nitrogen species during TPR. Upon further heating to 1258 K (J), β-$Mo_2N_{0.78}$ was again altered to molybdenum metal, which resulted in a large evolution of nitrogen gas in the range of 1050 to 1258 K. Thus, the peak at 1156 K for NH-H was due to nitrogen desorption from the reduction of β-$Mo_2N_{0.78}$ to molybdenum metal as similarly shown by the peak of 1197 K for NH-M. Boudart *et al.* (22, 27) studied nitrogen adsorption and ammonia decomposition on polycrystalline molybdenum and reported that the surface was predominantly covered with adsorbed nitrogen and some dissociated species. Haddix *et al.* (28) also reported that the decomposition of NH_3 adsorbed on γ-Mo_2N produced strongly adsorbed NH_2 and NH groups as well as N and H atoms after evacuation of adsorbed NH_3 at 573 K. The desorption of nitrogen gas was reported to proceed through the recombination of NH_x adsorbed on the surface with hydrogen above 645 K (28). Thus, NH_x species are created through the decomposition of ammonia fed through the cooling process after NH_3 treatment. During TPR, these NH_x species reacted with molybdenum oxides and metals to form γ-Mo_2N and β-$Mo_2N_{0.78}$.

He-Cooled Nitrided Catalyst

The structure and composition of the molybdenum compounds changed through purging at 973 K and cooling to room temperature in flowing helium (N in Fig. 4) after NH_3 treatment (D in Fig. 2). The TPR profiles of the HE catalysts are shown in Fig. 3. The TPR profiles of the HE-L and -M catalysts showed a large nitrogen desorption peak at 1179–1199 K, as shown in Figs. 3a and 3b. The XRD data on the HE catalysts indicated changes from MoO_2 to γ-Mo_2N on HE-L (K and L in Fig. 4) and from β-$Mo_2N_{0.78}$ to γ-Mo_2N on HE-M (N and O) during TPR. In contrast, no peaks of nitrogen desorption were observed at 800–1000 K during the

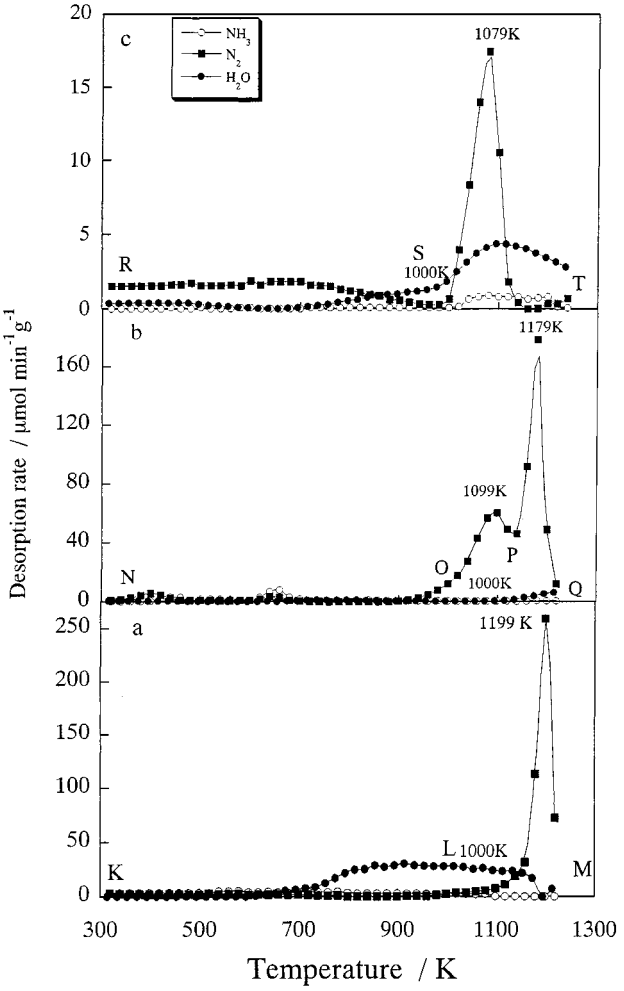

FIG. 3. N_2 desorption in TPR profiles of (a) HE-L, (b) HE-M, and (c) HE-H catalysts.

decomposition of NH_x adsorbed on molybdenum oxides and nitrides, as seen in the NH-L and -M catalysts, respectively. No ammonia was released for the TPR profiles of the HE catalysts. The desorption of ammonia during TPR is due to nitrogen adsorbed on the surface reacting with hydrogen (21–27). Therefore, purging and cooling of the NH_3-treated catalyst with helium removed adsorbed NH_x from the surface and diffused nitrogen atoms from the bulk, as in HE-M, leading to the change from γ-Mo_2N to β-$Mo_2N_{0.78}$. The HE catalyst is annealed to form β-$Mo_2N_{0.78}$ from γ-Mo_2N during the loss of nitrogen, whereas the NH catalyst remains as γ-Mo_2N in the presence of NH_3. The nitrogen desorption at 1099 and 1179 K for HE-M during TPR led to the corresponding structural changes of γ-Mo_2N to β-$Mo_2N_{0.78}$ and β-$Mo_2N_{0.78}$ to molybdenum metal (O–P and P–Q in Fig. 4), respectively, in agreement with those of the NH-L and -M catalysts. For the HE-H catalyst, the nitrogen peak temperature shifted to about 100 K lower than that for the NH-H catalyst during the transformation of β-$Mo_2N_{0.78}$ into molybdenum metal and was not observed below 1000 K. The amount of nitrogen desorption from HE-H was less than that of NH-H. Since the XRD showed the presence of molybdenum metal together with small portions of β-$Mo_2N_{0.78}$ at 1000 K (S in Fig. 4), purging of the HE-H catalyst with helium at 973 K did not fully remove the NH_x species after NH_3 treatment. Furthermore, the crystallite sizes of the molybdenum nitrides were 2.71 and 3.27 nm for NH-M and HE-M, respectively, with the NH-M having the smallest particle size of the catalysts, as shown in Table 1. The HE catalysts had larger crystallite sizes than the NH catalysts. The HE catalysts have smaller surface areas than the NH catalysts, consistent with the hypothesis of large particles. We believe that the large crystallite size of the molybdenum oxide, nitride, and metal particles was due to purging and cooling to room temperature in flowing helium.

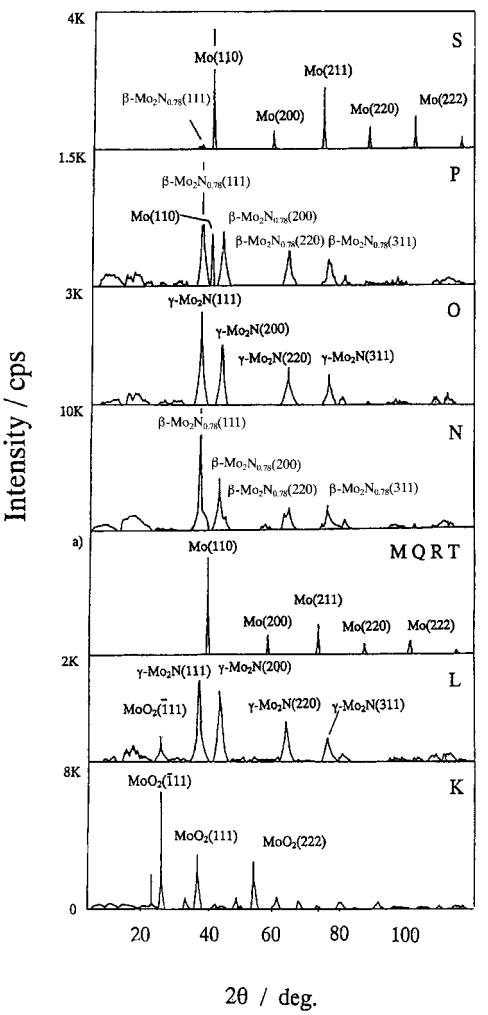

FIG. 4. The XRD spectra of the (K, N, Q) as-prepared, (L, O, R) intermediates of, and (M, P, S) final compounds of HE-L, HE-M, and HE-H catalysts during TPR, respectively. (a) 20 K for M, 6 K for Q, 10 K for R, and 12 K for T.

CO Adsorption

The amount of irreversible CO uptake for NH-M was 1.47×10^{14} molecules cm^{-2}, which was 4 times greater than that for HE-M, as shown in Table 1. Volpe and Boudart (29) reported that the uptake of irreversible CO on the 975 K nitrided MoO_3 was 2.6×10^{14} molecules cm^{-2}. A recent study of molybdenum oxynitride gave similar CO irreversible uptake values of 1.4×10^{14} molecules cm^{-2} (27). Oyama and co-workers also reported that γ-Mo_2N was prepared with 1.9×10^{14} molecules cm^{-2} (30), although commercial Mo_2N had a CO site density of 0.84×10^{14} molecules cm^{-2} (1). Thus, the CO uptake of the NH-M catalyst obtained was similar to that of commercial Mo_2N and was consistent with the CO uptakes reported by other authors (1, 29, 30). The ratio of irreversible to total CO uptake was 0.47 and 0.52 for the molybdenum nitrides (NH-M and HE-M, respectively). These values were also smaller than that obtained by Volpe and Boudart of 0.67 (29).

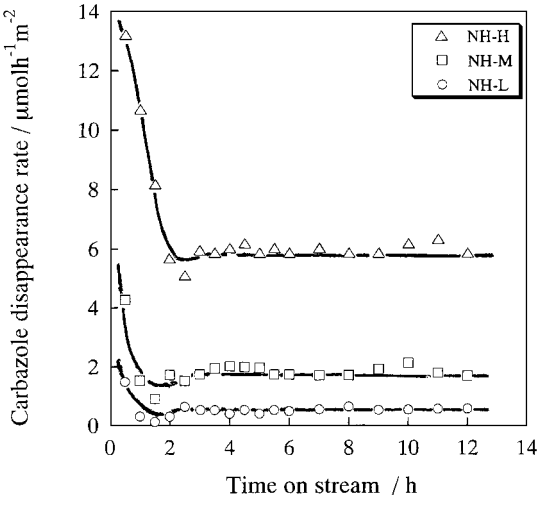

FIG. 5. Variation in HDN of carbazole for (○) NH-L, (□) NH-M, and (△) NH-H catalysts with time-on-stream at 573 K and 10.1 MPa.

HDN Activity

The main denitrogenated product was bicyclohexyl with a small amount of cyclohexylhexene. The primary hydrogenated product was tetrahydrocarbazole in the reaction products (4). Hydrogenated carbazole compounds such as hexahydrocarbazole and octahydrocarbazole were barely observed as reaction products with the exception of a relatively high amount of tetrahydrocarbazole. The time dependence of the disappearance rate of carbazole HDN on the catalysts was measured for the catalysts. Shown in Fig. 5 is the disappearance rate of carbazole HDN on the NH-L, -M, and -H catalysts as a function of time on stream at 573 K. The reaction reached steady state at 4 h after the feed was introduced into the reactor. The NH-H was expected to shrink and sinter as a result of NH_3 treatment at 1173 K, showing the highest HDN rate in carbazole HDN. The NH-M catalyst showed the medium activity of the catalysts. For the HE catalysts, the same trend was observed. The rates for the C–N hydrogenolysis and hydrogenation during the HDN of carbazole after 8–12 h are given in Table 3. The NH-M and HE-M catalysts showed the highest activity while the NH-H and HE-H catalysts exhibited the second greatest activity for C–N hydrogenolysis. In contrast, perhydrocarbazole was formed in a relatively high amount for the NH-H and HE-H catalysts, indicating a high selectivity for hydrogenation, compared to that for NH-M and HE-M. Both the NH-H and HE-H catalysts, which contained molybdenum metal (main phase (110)), were the most active during the hydrogenation of carbazole. For the NH-L and HE-L catalysts, MoO_2 was much less active than the other molybdenum species for the C–N hydrogenolysis and hydrogenation in carbazole HDN.

The turnover frequency for C–N hydrogenolysis and hydrogenation over HE-M per CO uptake was 0.309 and 0.908 mmol mol CO^{-1} s^{-1}, respectively. For the hydrogenation of carbazole, the TOF of HE-H was 2.42 mmol mol CO^{-1} s^{-1}. Since the CO uptake was unexpectedly greater for the NH catalyst because of the surface ammonia reacting to form amides, the TOF was not evaluated for the NH catalysts. Thompson *et al.* (6, 31) prepared unsupported molybdenum nitride for the temperature-programmed reaction of MoO_3 with ammonia at SV of 17 and 8.5 h^{-1} (under

TABLE 3

HDN of Carbazole at 573 K and 10.1 MPa

Catalyst NH_3 treating temperature (K)	C–N hydrogenolysis[a]			Hydrogenation[b]		
	NH (μmol h^{-1} m^{-2})	HE (μmol h^{-1} m^{-2})	HE (mmol mol CO^{-1} s^{-1})	NH (μmol h^{-1} m^{-2})	HE (μmol h^{-1} m^{-2})	HE (mmol mol CO^{-1} s^{-1})
773	0.033	0.036	0.047	0.55	0.35	0.46
973	0.789	0.674	0.309	1.00	1.98	0.908
1173	0.248	0.197	0.076	6.24	6.28	2.42

[a] Based on the formation of the denitrogenated compounds.
[b] Based on the formation of the hydrogenated compounds.

our conditions, SV of 3822 h^{-1}) and reported that the TOF was 0.36 and 1.02 mmol mol O_2^{-1} s^{-1}, respectively, for pyridine HDN at 633 K and 101 kPa total pressure. These values are comparable with the results measured by CO adsorption for the HDN of carbazole, even though it is difficult to reduce carbazole, one of the three-ring nuclear nitrogen compounds.

Mo Species and Nitrogen Desorption during TPR

During the TPR run, molybdenum oxide in the as-prepared NH-L catalyst reacted with adsorbed NH_x to form γ-Mo_2N and β-$Mo_2N_{0.78}$, together with desorbing ammonia and nitrogen in the process. The adsorbed NH_x species were formed in the decomposition of ammonia during the cooling with ammonia from treating temperature to room temperature. Purging of the catalyst with helium at 973 K after NH_3 treatment caused a change in the structure of the molybdenum nitride from γ-Mo_2N to β-$Mo_2N_{0.78}$ for HE-M. The nitrogen desorption from the molybdenum species was deconvoluted to four parts and is shown in Fig. 6 and Table 2. The nitrogen desorption was assigned to (1) the release of NH_x species adsorbed on MoO_2 at 875 K, (2) the release of NH_x species adsorbed on γ-Mo_2N at 940 K, (3) the transformation of γ-Mo_2N into β-$Mo_2N_{0.78}$ at 1070–1095 K, and (4) the reduction of β-$Mo_2N_{0.78}$ to molybdenum metal at 1165–1250 K. For the HE catalysts, nitrogen desorbed from the surface and the bulk was less than that for the NH catalyst. Purging the NH_3-treated catalysts with helium lowered the number of surface NH_x species adsorbed on the catalyst and nitrogen dissolved in the bulk, leading to an alteration of the structure of the molybdenum compounds. The amounts of N_2 desorption for NH-M between 1017 and 1158 K and between 1158 and 1257 K were 199 and 321 μmol g^{-1}, respectively. The amount of nitrogen (N_2) desorption was stoichiometrically calculated to be 0.371, 1.31, and 1.69 mmol g^{-1} in the transformation of γ-Mo_2N into β-$Mo_2N_{0.78}$, β-$Mo_2N_{0.78}$ into Mo metal, and γ-Mo_2N into MoO_2, respectively, based on total conversion of the 97.1% samples to the resulting products. From the results, 53.6% of γ-Mo_2N was altered to β-$Mo_2N_{0.78}$ and 24.5% of β-$Mo_2N_{0.78}$ to Mo metal for NH-M. For HE-M, 212% of γ-Mo_2N was converted to β-$Mo_2N_{0.78}$ and 38.6% of β-$Mo_2N_{0.78}$ to Mo metal. This result indicated that a large number of surface NH_x species adsorbed on the surface of the NH-M catalyst. Balandin and Rozhdestvenskaya (32) reported that molybdenum dioxide adsorbed 1.89 mmol g-MoO_2^{-1} of nitrogen in 10 h at 773 K and further, 2.67 mmol g-MoO_2^{-1} of N_2 in the same period at 797 K. Furthermore, Aika and Ozaki (33) reported that 1.92 mmol g-Mo^{-1} of N_2 was adsorbed on a reduced molybdenum metal after 69 h of nitriding in N_2 at 775 K. The NH-L and HE-L catalysts contained 0.459 and 0.557 mmol g^{-1} of N_2, respectively, corresponding to 24.3 and 29.5% of nitrogen desorption obtained from Balandin and Rozhdestvenskaya (32). The long duration period (1 h) in purging with helium after NH_3 treatment affected the nitrogen content of the catalysts.

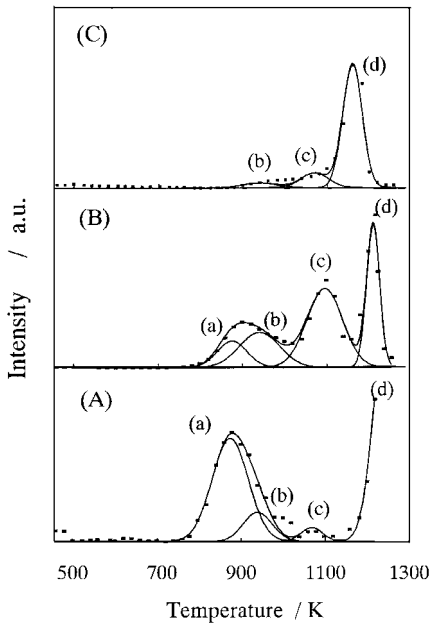

FIG. 6. The nitrogen desorption in TPR profiles over the (A) NH-L, (B) NH-M, and (C) NH-H catalysts.

Mo Species and HDN Activity

The NH-M catalyst showed the highest activity and the HE-M catalyst followed, while the NH-L and HE-L catalysts exhibited the lowest activity for C–N hydrogenolysis during the HDN of carbazole. The XRD analysis showed the presence of γ-Mo_2N, β-$Mo_2N_{0.78}$, and MoO_2 in NH-M, HE-M, and NH(HE)-L, respectively. γ-Mo_2N was the most active for the C–N hydrogenolysis of carbazole, followed by β-$Mo_2N_{0.78}$ and MoO_2. In contrast, the rates of the hydrogenation of carbazole on NH-H and HE-H were markedly greater than those of the L and M catalysts. Both the NH-H and HE-H catalysts, which contained molybdenum metal (main phase (110) in Figs. 2 and 4), were the most active during the hydrogenation of carbazole. From these results, molybdenum metal showed the highest activity for the hydrogenation of carbazole. For the NH-L and HE-L catalysts, MoO_2 was much less active than the other molybdenum species for C–N hydrogenolysis and hydrogenation. Thus, the activities of each molybdenum species for C–N hydrogenolysis and hydrogenation, especially molybdenum nitrides and metals, must be compared with the surface and bulk properties.

The NH-M and -H catalysts with smaller particle and crystallite sizes were more active than those of the HE-M and -H catalysts for C–N hydrogenolysis, respectively, while the HE-L catalyst did not follow suit, as shown in Table 1. The smaller crystallites and particles of molybdenum

nitrides and metals were involved in the C–N hydrogenolysis. Furthermore, correlating the surface grain boundary length of the unsupported molybdenum nitride catalysts with the activity for pyridine HDN, the HDN rate was proportional $d_p d_c^{-2}$ (31), as shown in Table 1. In our study, the surface grain boundary lengths of all catalysts were not correlated with the activities for the C–N hydrogenolysis but those for the hydrogenation in Tables 1 and 3. Therefore, the C–N hydrogenolysis occurred on smaller particles and crystallites, such as at the edge and corner sites of molybdenum nitrides and metals, whereas the hydrogenation is favored on the surface grain boundary of the large molybdenum compound particles.

Nitrogen-deficient sites would be created on the molybdenum nitrides with a small N/Mo ratio. The NH-M catalyst (molybdenum nitride) with a low N/Mo ratio was more active for the C–N hydrogenolysis than the HE-M catalyst with a high N/Mo ratio, although this was not true for the 773 and 1173 K treated catalysts. This indicated that the C–N hydrogenolysis sites were located at the nitrogen-deficient sites of the molybdenum nitrides. For the hydrogenation of carbazole, however, there is no observable relationship between the hydrogenation activity and N/Mo ratio. Thompson *et al.* (6) also reported that the HDN activity increased as the N/Mo ratio decreased during the HDN of pyridine on 4–16% Mo loaded alumina-supported nitride catalysts, suggesting that the most active sites were located at the nitrogen deficient sites near the perimeters of the two-dimensional, raftlike domains. Lower active sites for hydrogenation were associated with the γ-Mo_2N crystallite surface.

A number of adsorption methods have been used to characterize the active sites on molybdenum catalysts (6, 29, 30, 31, 34). The HDN activity of the unsupported and alumina-supported molybdenum nitride catalysts was reported to linearly increase with the amount of NH_3 chemisorbed in NH_3-TPD (13, 35), indicating that the acid sites are related to the HDN reaction. Since ammonia was used in the cooling after NH_3 treatment, in this study, the ammonia and decomposed ammonia (adsorbed NH_x) were monitored for studying the active sites instead of the traditional NH_3-TPD method. An attempt was made to correlate nitrogen desorption with the activities for C–N hydrogenolysis and hydrogenation for the NH catalysts. The HE catalysts could not be used because adsorbed nitrogen species on the surface or sublayer molybdenum nitrides were not stable to purging the nitride catalysts. The data in Table 2 are plotted versus the rates for C–N hydrogenolysis and hydrogenation in Fig. 7. Figure 7A indicated a linear relationship between the rate of C–N hydrogenolysis and the amount of nitrogen desorbed from the γ-Mo_2N surface (b). The nitrogen desorption was likely to be due to NH_x adsorbed on the active sites, such as acid sites and coordinatively unsaturated sites. Hence, the active sites for the C–N hydrogenolysis were closely related to the coordinatively unsaturated molybdenum sites, i.e., nitrogen-deficient sites on small particles and crystallites of molybdenum nitrides. On the other hand, as shown in Fig. 7B, the nitrogen desorption for the NH catalysts is plotted versus the hydrogenation rate. The amounts of nitrogen desorption (c) and (d) were related with the hydrogenation rates in carbazole HDN. The nitrogen desorptions (c) and (d) were due to the transformation of γ-Mo_2N into β-$Mo_2N_{0.78}$ and the reduction of β-$Mo_2N_{0.78}$ to molybdenum metal, respectively. It is concluded that the hydrogenation sites were located at the surface grain boundary of the

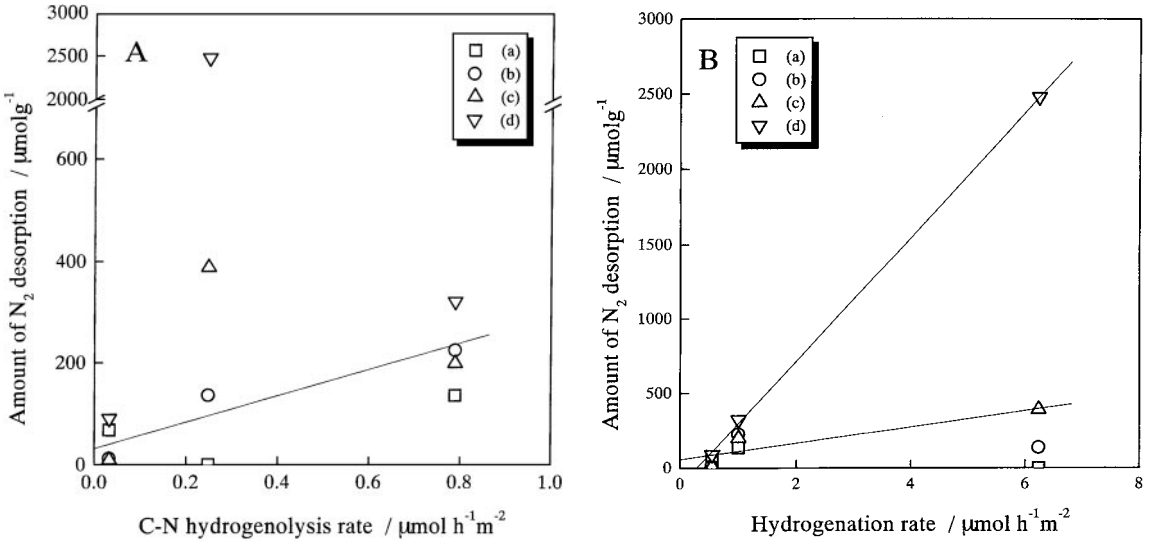

FIG. 7. Rates of (A) C–N hydrogenolysis and (B) hydrogenation in the HDN of carbazole vs four kinds of nitrogen desorption from the NH catalysts.

molybdenum metal crystallites and molybdenum nitrides. The surface grain boundary of molybdenum metal (110) was responsible for high activity for the hydrogenation of carbazole.

CONCLUSIONS

(1) The NH catalysts had a higher surface area than the HE catalysts at the same NH_3 treating temperature. Cooling of the NH_3-treated catalysts in a stream of ammonia results in smaller particles and better heterogeneity of the surface than that in a stream of helium. NH_3 treatment at high temperature lowered the surface area of the catalysts due to catalyst sintering.

(2) NH_x species were present on the nitrided catalysts and reacted with molybdenum oxides and metal to form γ-Mo_2N and β-$Mo_2N_{0.78}$, respectively, during TPR.

(3) The nitrogen desorption from the nitrided catalyst during TPR was attributed to four species: (1) The N_2 peaks at 875 and 940 K for the release of nitrogen gas desorbed from the reaction and recombination of NH_x adsorbed on MoO_2, and (2) on γ-Mo_2N, and (3) the peaks at 1070–1095 and 1165–1250 K for the release of nitrogen gas from (4) the transformation of γ-Mo_2N into β-$Mo_2N_{0.78}$ and the reduction from β-$Mo_2N_{0.78}$ to molybdenum metal.

(4) Purging of the NH_3-treated catalysts with helium at 973 K removed adsorbed nitrogen species except for the transformation of γ-Mo_2N into β-$Mo_2N_{0.78}$ at 1070–1095 K and the reduction of β-$Mo_2N_{0.78}$ to molybdenum metal at 1165–1250 K.

(5) The activity of the Mo species for C–N hydrogenolysis of carbazole decreased in the following order:

$$\gamma\text{-}Mo_2N > \beta\text{-}Mo_2N_{0.78} \gg \text{Mo metal} > MoO_2.$$

The C–N hydrogenolysis occurs on the nitrogen deficient sites of small particles and crystallites of molybdenum nitrides of NH-M and HE-M.

(6) The activity of the Mo species for hydrogenation of carbazole decreased in the following order:

$$\text{Mo metal} \gg \beta\text{-}Mo_2N_{0.78} > \gamma\text{-}Mo_2N > MoO_2.$$

The hydrogenation of carbazole takes place on the surface grain boundary of molybdenum metal of NH-H and HE-H.

ACKNOWLEDGMENTS

This work has been carried out as a research project of The Japan Petroleum Institute commissioned by the Petroleum Energy Center with the support of the Ministry of International Trade and Industry. We are grateful for the Grant-in-Aid for Scientific Research of the Ministry of Education Grant (09555244).

REFERENCES

1. Schlatter, J. C., Oyama, S. T., Metcalfe, J. E., III, and Lambert, J. M., Jr., *Ind. Eng. Chem. Res.* **27**, 1648 (1988).
2. Ramanathan, S., and Oyama, S. T., *J. Phys. Chem.* **99**, 16365 (1995).
3. Lee, K. S., Abe, H., Reimer, J. A., and Bell, A. T., *J. Catal.* **139**, 34 (1993).
4. Choi, J.-G., Curl, R. L., and Thompson, L. T., *J. Catal.* **146**, 218 (1994).
5. Sajkowski, D. J., and Oyama, S. T., *Appl. Catal. A* **134**, 339 (1996).
6. Colling, C. W., and Thompson, L. T., *J. Catal.* **146**, 193 (1994).
7. Nagai, M., and Miyao, T., *Catal. Lett.* **15**, 105 (1992).
8. Lee, K. S., Abe, H., Reimer, J. A., and Bell, A. T., *J. Catal.* **139**, 34 (1993).
9. Raje, A., Liaw, S.-J., Chary, K. V. R., and Davis, B. H., *Appl. Catal. A* **123**, 229 (1995).
10. Dolce, G. M., Savage, P. E., and Thompson, L. T., *Energy Fuels* **11**, 668 (1997).
11. Markel, E. J., and Van Zee, J. W., *J. Catal.* **126**, 643 (1990).
12. Nagai, M., Miyao, T., and Tsuboi, T., *Catal. Lett.* **18**, 9 (1993).
13. Nagai, M., Miyata, A., Kusagaya, T., and Omi, S., *in* "The Chemistry of Transition Metal Carbides and Nitrides" (S. T. Oyama, Ed.), Chap. 17. Blackie, London, 1996.
14. Miyata, A., Omi, S., and Nagai, M., *J. Jpn. Petrol. Inst.* **38**, 251 (1995).
15. Nagai, M., Kusagaya, T., Miyata, A., and Omi, S., *Bull. Soc. Chim. Belg.* **104**, 311 (1995).
16. Nagai, M., Miyata, A., Miyao, T., and Omi, S., *J. Petrol. Inst. Jpn.* **40**, 500 (1997).
17. Fastrup, B., Muhler, M., Nielsen, H. N., and Nielsen, L. P., *J. Catal.* **142**, 135 (1993).
18. Koerts, T., Welters, W. J. J., and van Santen, R. A., *J. Catal.* **134**, 1 (1992).
19. Wei, Z., Xin, Q., Grange, P., and Delmon, B., *J. Catal.* **168**, 176 (1997).
20. Nagai, M., Masunaga, T., and Hanaoka, N., *J. Catal.* **101**, 284 (1986).
21. Haddix, G. W., Reimer, J. A., and Bell, A. T., *J. Catal.* **108**, 50 (1987).
22. Boudart, M., Egawa, C., Oyama, S. T., and Tamaru, K., *J. Chim. Phys.* **78**, 987 (1981).
23. Boudart, M., and Dje'ga-Mariadassou, G., *in* "Kinetics of Heterogeneous Catalytic Reactions," p. 163. Princeton Univ. Press, Princeton, NJ, 1984.
24. Thomas, J. M., and Thomas, W. J., *in* "Principles and Practice of Heterogeneous Catalysis," p. 548. VCH, New York, 1997.
25. Matsushita, K., and Hansen, R. S., *J. Chem. Phys.* **54**, 2278 (1971).
26. Eley, D. D., and Russell, S. H., *Proc. Roy. Soc. London A* **341**, 31 (1974).
27. Oyama, S. T., and Boudart, M., *J. Res. Inst. Catal. Hokkaido Univ.* **28**, 305 (1980).
28. Haddix, G. W., Jones, D. H., Reimer, J. A., and Bell, A. T., *J. Catal.* **112**, 556 (1988).
29. Volpe, L., and Boudart, M., *J. Solid State Chem.* **59**, 332 (1985); *J. Phys. Chem.* **90**, 4874 (1986).
30. Oyama, S. T., Schlatter, J. C., Metcalfe, J. E., III, and Lambert, J. M., Jr., *Ind. Eng. Chem. Res.* **27**, 1639 (1988).
31. Choi, J.-G., Brenner, J. R., Colling, C. W., Demczyk, B. G., Dunning, J. L., and Thompson, L. T., *Catal. Today* **15**, 201 (1992).
32. Balandin, A. A., and Rozhdestvenskaya, I. D., *Bull. Acad. Sci. U.S.S.R. Div. Chem. Sci.*, 1804 (1959).
33. Aika, K., and Ozaki, A., *J. Catal.* **14**, 311 (1969).
34. Demczyk, B. G., Choi, J.-G., and Thompson, L. T., *Appl. Surf. Sci.* **78**, 63 (1994).
35. Colling, C. W., Choi, J.-G., and Thompson, L. T., *J. Catal.* **160**, 35 (1996).